J Stat Phys (2010) 139: 333–344
DOI 10.1007/s10955-010-9943-6

Mixed-Spin Ising Model in an Oscillating Magnetic Field and Compensation Temperature

Mustafa Keskin · Mehmet Ertaş

Received: 2 October 2009 / Accepted: 3 March 2010 / Published online: 17 March 2010

Abstract Godoy et al. (Phys. Rev. B 69, 054428, 2004) presented a study of the magnetic properties of a mixed spin (1/2, 1), Ising ferrimagnetic model on a hexagonal lattice without an oscillating magnetic field. They employed dynamic mean-field calculations and Monte Carlo simulations to find the compensation point of the model and to present the phase diagrams. It has been found that the N-type compensation temperature appears only when the intrasublattice interaction between spins in the σ sublattice is ferromagnetic. Moreover, the system only undergoes a second-order phase transition. In this work, we extend the study a dynamic compensation temperature of a mixed spin-1/2 and spin-1 Ising ferrimagnetic system on a hexagonal lattice in the presence of oscillating magnetic field within the framework of dynamic mean-field calculations. We find that the system displays the N-type compensation temperature. We also calculate dynamic phase diagrams in which contain the paramagnetic, ferrimagnetic, nonmagnetic fundamental phases and two different mixed phases, depending on the interaction parameters and oscillating magnetic field. The system also exhibits tricritical and reentrant behaviors.

Keywords Mixed-spin Ising system · Dynamic phase transitions · Dynamic compensation temperature · Dynamic phase diagrams · Glauber-type stochastic dynamics

1 Introduction

Godoy et al. [1] presented a study of the magnetic properties of a mixed spin (1/2, 1) Ising ferrimagnetic model on a hexagonal lattice without an oscillating magnetic field within the framework of dynamic mean-field calculations and Monte Carlo simulations. They found the compensation point of the model and presented the phase diagrams. This work is important due to the reasons that it is dealing the ferrimagnetisms and as well as the compensation temperature. The phenomenon of ferrimagnetisms has been one of the intensively studied subjects in statistical mechanics and condensed matter physics, because of their potential

M. Keskin (✉) · M. Ertaş
Department of Physics, Erciyes University, 38039 Kayseri, Turkey
e-mail: keskin@erciyes.edu.tr

device applications in technologically important materials [2]. It should be mentioned that the equilibrium properties of the mixed spin-1/2 and spin-1 Ising system have been studied by the well known methods in equilibrium statistical physics, such as the mean-field approximation (MFA), the effective-field theory (EFT), the Monte Carlo (MC) simulations, the renormalization-group (RG) calculation and the exact formulation on the Bethe lattice using the exact recursion equations ([3–7] and references therein). In contrast to ferromagnets and antiferromagnets, there is in ferrimagnets an important possibility of the existence, under certain conditions, of a compensation temperature where the total magnetization vanishes below the critical temperature. The existence of compensation temperatures is of great technological importance, since at this point only a small driving field is required to change the sign of the total magnetization. This property is very useful in thermomagnetic recording, electronic and computer technologies [8–10]. The presence of the static compensation temperature in the mixed spin-1/2 and spin-1 Ising system has been studied by using a variety of techniques, such as the MFA, the EFT, the MC simulations ([11–13] and references therein). While the static compensation temperature in the mixed spin (1/2, 1) system has been studied in detail, the dynamic compensation temperature of this system has not been as thoroughly explored. An early attempt to study the dynamic compensation temperature in the system was made by Godoy et al. [1] who studied the dynamic compensation temperature in the mixed spin (1/2, 1) system on a hexagonal lattice without an oscillating magnetic field. The purpose of this paper is to extend the work of Godoy et al. [1], i.e. the study a dynamic compensation temperature of a mixed spin-1/2 and spin-1 Ising ferrimagnetic system on a hexagonal lattice in the presence of oscillating magnetic field within the framework of dynamic mean-field calculations. Especially, time variations of the average sublattice magnetizations are studied to find the phases in the system, the temperature dependence of the dynamic sublattice magnetizations, and the total dynamic magnetization are investigated to determine the compensation temperature and dynamic phase transitions (DPT) points, respectively. The dynamic phase diagrams including the compensations temperatures are presented in five different planes.

The organization of the remaining part of this paper is as follows. In Sect. 2, the model and its formulations, namely the derivation of the set of mean-field dynamic equations, are briefly given by using Glauber-type stochastic dynamics in the presence of a time-dependent oscillating external magnetic field. The detailed numerical results and discussions are presented in Sect. 3, followed by a brief summary.

2 Model and Formulations

The considered model is a mixed spin-1/2 and spin-1 Ising ferrimagnetic system on a hexagonal lattice under the oscillating magnetic field. The lattice is formed by alternate layers of σ and S spins; hence the two different types of spins are described by Ising variables, which can take the values $\sigma = \pm 1/2$, and $S = \pm 1, 0$. σ and S spins are distributed in alternate layers of a hexagonal lattice, seen in Fig. 1. The Hamiltonian model for the system is

$$\mathcal{H} = -J_1 \sum_{\langle ij \rangle} \sigma_i S_j - J_2 \sum_{\langle ij \rangle} \sigma_i \sigma_j - J_3 \sum_{\langle ij \rangle} S_i S_j - D \sum_j S_j^2 - H \left(\sum_i \sigma_i + \sum_j S_j \right), \quad (1)$$

where the summation index $\langle ij \rangle$ denotes a summation over all pairs of nearest-neighbor spins. J_1, J_2 and J_3 are the exchange couplings between the nearest-neighbor pairs of spins σ–S, σ–σ and S–S, respectively. It is seen from Fig. 1, J_1 interaction restricted to the

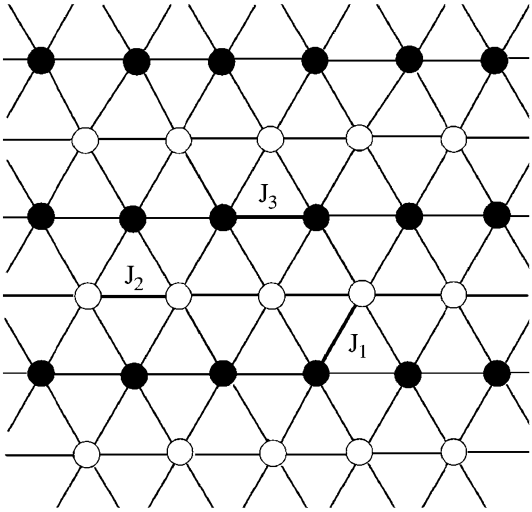

Fig. 1 The sketch of the spin arrangement on the hexagonal lattice. The lattice is formed by alternate layers of σ (*open circles*) and S (*solid circles*) spins

z_1 nearest-neighbor pair of spins that $z_1 = 4$, and J_2 and J_3 restricted to the coordination numbers of z_2 and z_3, respectively, in which $z_2 = z_3 = 2$. The parameter J_1 will be taken negative in all the subsequent analyses, that is, the intersublattice coupling is antiferromagnetic to have a simple but an interesting model of a ferrimagnetic system. $D$is the crystal-field interaction or a single-ion anisotropy constant, and H is the oscillating magnetic field: $H(t) = H_0 \cos(wt)$, with H_0 and $w = 2\pi\nu$ being the amplitude and the angular frequency of the oscillating field, respectively. The system is in contact with an isothermal heat bath at an absolute temperature T_A.

Now, we apply the Glauber-type stochastic dynamics [14] to obtain the set of the mean-field dynamic equations. Since the derivation of the mean-field dynamic equations was described in detail for this mixed-spin system [1] and different mixed-spin systems [1, 15–17], in here, we shall only give a brief summary. If the S-spins momentarily fixed, the master equation for σ-spins can be written as

$$\frac{d}{dt}P(\sigma_1, \sigma_2, \ldots, \sigma_N; t) = -\sum_i W_i(-\sigma_i)P(\sigma_1, \sigma_2, \ldots, \sigma_i, \ldots, \sigma_N; t) + \sum_i W_i(\sigma_i)P(\sigma_1, \sigma_2, \ldots, -\sigma_i, \ldots, \sigma_N; t), \tag{2}$$

where $W_i(\sigma_i)$ is the probability per unit time that ith σ spin changes from σ_i to $-\sigma_i$. Since the system is in contact with a heat bath at absolute temperature T_A, each spin σ can flip with the probability per unit time by the Boltzmann factor;

$$W_i(\sigma_i) = \frac{1}{\tau}\frac{\exp(-\beta\Delta E(\sigma_i))}{\sum_{\sigma_i}\exp(-\beta\Delta E(\sigma_i))}, \tag{3}$$

where $\beta = 1/k_B T_A$, k_B is the Boltzmann constant, the sum ranges the two possible values $\pm 1/2$ for σ_i and

$$\Delta E(\sigma_i) = 2\sigma_i\left(H + J_1\sum_j S_j + J_2\sum_j \sigma_j\right), \tag{4}$$

gives the change in the energy of the system when the σ_i-spin changes. The probabilities satisfy the detailed balance condition. Using (2), (3), (4) with the mean-field approach, we obtain the mean-field dynamic equation for the σ-spins as

$$\Omega \frac{d}{d\xi} m_\sigma = -m_\sigma + \frac{1}{2} \tanh[\beta(2J_1 m_S + J_2 m_\sigma + H_0 \cos(\xi))], \tag{5}$$

where $m_\sigma = \langle \sigma \rangle$, $m_S = \langle S \rangle$, $\xi = wt$, and $\Omega = \tau w = w/f$, w is the frequency of the oscillating magnetic field and f represents the frequency of spin flipping.

Now assuming that the σ-spins remain momentarily fixed and that the S-spins change, we obtain the mean-field dynamical equation for the S-spins by using the similar calculations as before, except we take $S = \pm 1, 0$ instead of $\sigma = \pm 1/2$. The second mean-field dynamic equation for S-spins is obtained as

$$\Omega \frac{d}{d\xi} m_S = -m_S + \frac{2\sinh[2\beta(2J_1 m_\sigma + J_3 m_S + H_0 \cos(\xi))]}{2\cosh[2\beta(2J_1 m_\sigma + J_3 m_S + H_0 \cos(\xi))] + \exp(-\beta D)}, \tag{6}$$

where $m_\sigma = \langle \sigma \rangle$, $m_S = \langle S \rangle$, $\xi = wt$, and $\Omega = \tau w$. Hence, a set of mean-field dynamical equations of the system are obtained. It should be mentioned that the set of dynamic mean-field equations, (5) and (6), is the same (with allowance for different notations and the oscillating magnetic field, H, is zero) as (18) and (19) in [1]. We fixed $J_1 = -1$ that the intersublattice interaction is antiferromagnetic and $\Omega = 2\pi$. We give the solution and discussion of these dynamic equations in the next section.

3 Numerical Results and Discussions

In this section, first the time variations of the average sublattice magnetizations are studied to find the phases in the system. In order to investigate the behaviors of time variations of the average sublattice magnetizations, first we have to study the stationary solutions of the set of coupled mean-field dynamical equations given in (5) and (6) when the parameters T, J_2, J_3, D and H_0 are varied. The stationary solutions of these equations will be periodic function of ξ with period 2π; that is, $m_\sigma(\xi + 2\pi) = m_\sigma(\xi)$ and $m_S(\xi + 2\pi) = m_S(\xi)$. Moreover, they can be one of three types according to whether they have or do not have the properties

$$m_\sigma(\xi + \pi) = -m_\sigma(\xi) \quad \text{and} \quad m_S(\xi + \pi) = -m_S(\xi). \tag{7}$$

The first type of solution satisfies (7) is called a symmetric solution. It corresponds to a paramagnetic (p) phase. In this solution, the sublattice average magnetizations $m_\sigma(\xi)$ and $m_S(\xi)$ are equal to each other. They oscillate around the zero value and are delayed with respect to the external magnetic field. The second type of solution, which does not satisfy (7), corresponds to a non-magnetic solution (nm). In this case, $m_\sigma(\xi)$ oscillates around the zero value and is delayed with respect to the external magnetic field and $m_S(\xi)$ does not follow the external magnetic field anymore, but instead of oscillating around a zero value, it oscillates around a nonzero value. The third type of solution, which does not satisfy (7), is called a nonsymmetric solution that corresponds to a ferrimagnetic (i) solution. In this case the magnetizations do not follow the external magnetic field any more; $m_\sigma(\xi)$ and $m_S(\xi)$ oscillate around $\pm 1/2$ and ± 1, respectively, this corresponds to the ferrimagnetic (i) phase. These facts are seen explicitly by solving (5) and (6) within the Adams-Moulton predictor-corrector method for a given set of parameters and initial values. The solutions are presented

in Fig. 2. From Fig. 2, one can see that four different solutions, namely the p, nm and i fundamental phases or solutions, and one coexistence solution, namely the $i + p$ mixed phase in which i and p phases coexist exist in the system. In Fig. 2(a), only the symmetric solution is always obtained, hence we have a paramagnetic (p) solution, but in Fig. 2(b) and 2(c)

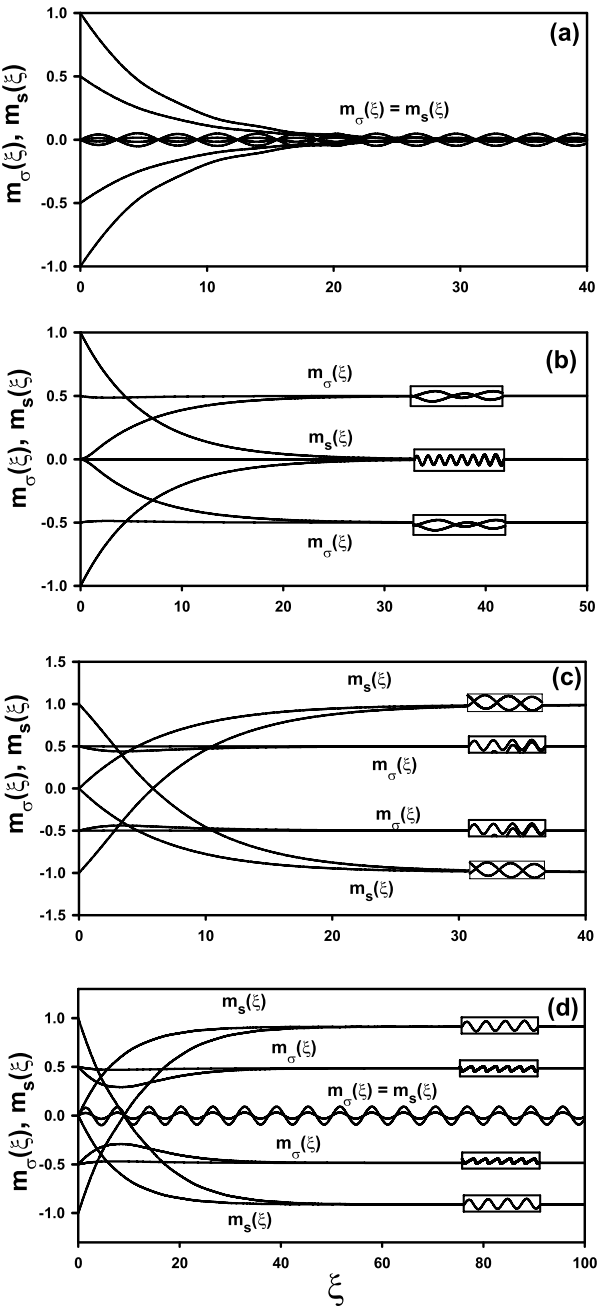

Fig. 2 Time variations of the average magnetizations ($m_\sigma(\xi)$ and $m_s(\xi)$): (**a**) Exhibiting a paramagnetic phase (p), $J_1 = -1.0$, $J_2 = 2.0$, $J_3 = 0.1$, $D = 3.0$, $H_0 = 2.0$ and $T = 5.0$. (**b**) Exhibiting a non-magnetic phase (nm), $J_1 = -1.0$, $J_2 = 5.0$, $J_3 = 0.9$, $D = -9.0$, $H_0 = 0.1$ and $T = 2.0$. (**c**) Exhibiting a ferrimagnetic phase (i), $J_1 = -1.0$, $J_2 = 5.0$, $J_3 = 0.9$, $D = 1.0$, $H_0 = 0.1$ and $T = 1.0$. (**d**) Exhibiting a coexistence region $(i + p)$, $J_1 = -1.0$, $J_2 = 1.1$, $J_3 = 0.9$, $D = -2.6$, $H_0 = 2.0$ and $T = 0.1$

only the non symmetric solutions are found; therefore, we have a ferrimagnetic (i) and a non-magnetic (nm) solutions, respectively. These solutions do not depend on the initial values. In Fig. 2(d), we have two solutions, namely i and p phases or solutions coexist in the system. The first solution, $m_\sigma(\xi)$ oscillates around $\pm 1/2$ values and $m_S(\xi)$ oscillates around ± 1 values; hence we have the i phase. The second one, $m_\sigma(\xi)$ and $m_S(\xi)$ oscillate around zero value and we have the paramagnetic (p) phase again. Therefore, we have the $i + p$ mixed phase or coexistence solution. In this case, the solution depend on the initial values. In addition to these three fundamental phases and a mixed phase, one more mixed phase, namely the $nm + p$ in which nm, p solutions coexist, exists in the system.

Then, the temperature dependence of the dynamic sublattice magnetizations and the total dynamic magnetization are investigated to determine DPT points and the compensation temperatures, respectively. This investigation leads us to obtain the DPT points and compensation temperatures. The dynamic sublattice magnetizations (M_σ, M_S) or the average sublattice magnetizations in a period and the dynamic total sublattice magnetization $M_t = (M_\sigma + M_S)/2$ are defined as

$$M_{\sigma,S} = \frac{1}{2\pi}\int_0^{2\pi} m_{\sigma,S}(\xi)d\xi, \tag{8a}$$

and

$$M_t = \frac{1}{2\pi}\int_0^{2\pi}\left(\frac{m_\sigma(\xi) + m_S(\xi)}{2}\right)d\xi. \tag{8b}$$

The behaviors of dynamic sublattice magnetizations (M_σ, M_S) and the dynamic total magnetization (M_t) as functions of the temperature for several values of interaction parameters are obtained by solving 8(a) and (b). We solve these equations by combining the numerical methods of the Adams-Moulton predictor corrector with the Romberg integration and the two explanatory and interesting examples are plotted in Figs. 3(a)–(d) in order to illustrate the calculation of the DPT points and the compensation temperatures. In these figures, T_c and T_t are the second-order and first-order phase transition temperatures, respectively. T_{comp} is the compensation temperature. Figure 3(a) shows the behavior of $|M_\sigma|$, $|M_S|$ and $|M_t|$ as functions of the temperature for $J_1 = -1.0$, $J_2 = 5.0$, $J_3 = -0.1$, $D = 0.1$ and $H_0 = 2.0$. $|M_\sigma| = 0.5$ and $|M_S| = 1.0$ at the zero temperature and they decrease to zero continuously until T_c as the temperature increases, hence a second-order phase transition occurs at $T_C = 3.13$. In this case, the dynamic phase transition is from the i phase to the p phase. Moreover, one compensation temperature or N-type behavior occurs in the system that exhibits the same behavior classified after the Néel theory [18] as the N-type behavior [19]. Figure 3(b) shows the behavior of the thermal variations of $|M_\sigma|$, $|M_S|$ and $|M_t|$ for $J_1 = -1.0$, $J_2 = 0.33$, $J_3 = 0.7$, $D = -4.5$ and $H_0 = 0.15$ for all initial values. In Fig. 3(b), $|M_\sigma| = 0.5$ and $|M_S| = 0.0$ at the zero temperature, $|M_S|$ always equal to zero and $|M_\sigma|$ decreases zero discontinuously as the temperature increases; hence, the system undergoes a first-order phase transition from the nm phase to the p phase at $T_t = 0.119$. Therefore, T_t is the first-order phase transition temperature where discontinuity or jump occurs. Figures 3(c) and 3(d) illustrate the thermal variations of $|M_\sigma|$, $|M_S|$ and $|M_t|$ for $J_1 = -1.0$, $J_2 = 0.2$, $J_3 = 0.1$, $D = 0.1$ and $H_0 = 2$ for various different initial values. The behavior of Fig. 3(c), is similar to Fig. 3(a); hence, the system undergoes a second-order phase transition from the i phase to the p phase at $T_c = 1.22$. In Fig. 3(d), the system undergoes two successive phase transitions: The first one is a first-order because a discontinuity occurs for the dynamic sublattice magnetizations at $T_t = 0.15$. Transition is from the p phase to the i phase. The second

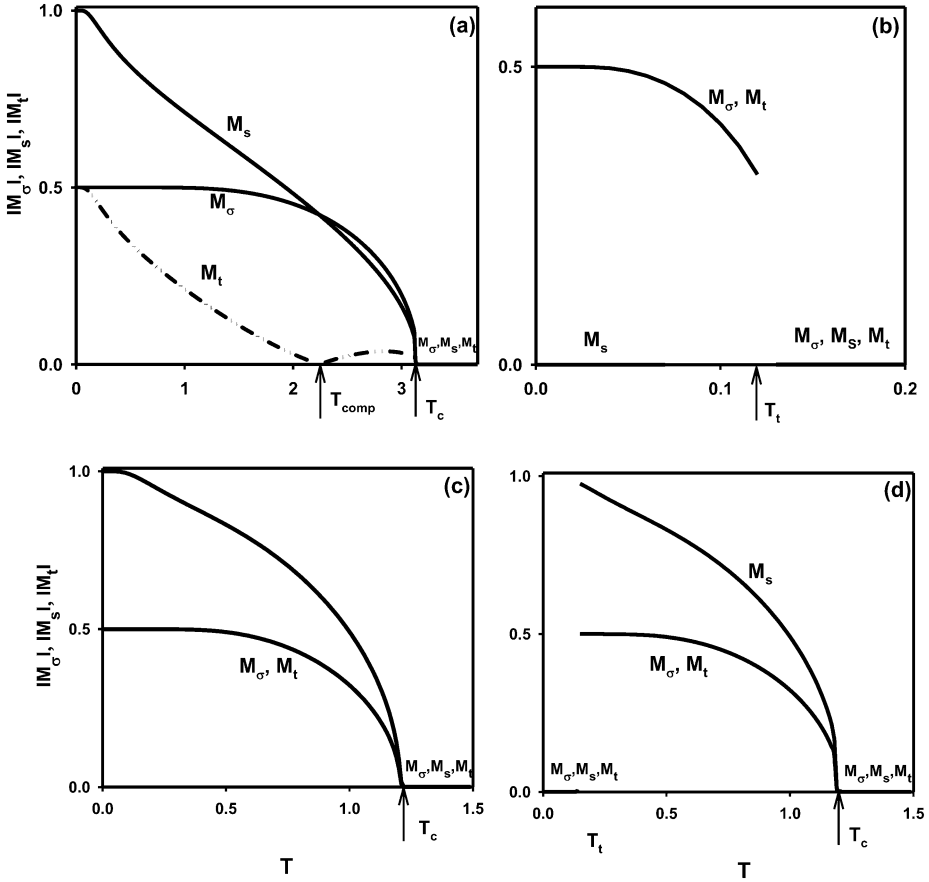

Fig. 3 The temperature dependence of the dynamic sublattice magnetizations ($|M_\sigma|, |M_S|$) and the total dynamic magnetization ($|M_t|$). T_c and T_t are the second- and first-order phase transition temperatures, respectively. (**a**) A second-order phase transition from the i phase to the p phase for $J_1 = -1.0$, $J_2 = 5.0$, $J_3 = 0.1$, $D = 0.1$ and $H_0 = 0.15$ and T_t is found 0.119. (**b**) A first-order phase transition from the *nm* phase to the p phase for $J_1 = -1.0$, $J_2 = 0.33$, $J_3 = 0.7$, $D = -4.5$ and $H_0 = 2$ and T_c is found 3.13. (**c**) A second-order phase transition from the i phase to the p phase for $J_1 = -1.0$, $J_2 = 0.2$, $J_3 = 0.1$, $D = 0.1$ and $H_0 = 2$ and the initial values of $|M_\sigma|$ and $|M_S|$ are taken one; T_c is found 1.22. (**d**) Two successive phase transitions, the first one is a first-order phase transition from the p phase to the i phase and the second one is a second-order phase transition the from the i phase to the p phase for $J_1 = -1.0$, $J_2 = 2.0$, $J_3 = 0.2$, $D = -1.5$ and $H_0 = 0.1$ and the initial values of $|M_\sigma|$ and $|M_S|$ are taken zero; T_c and T_t are found 1.22 and 0.15, respectively

one is a second-order phase transition from the i phase to the p phase at $T_c = 1.22$. This means that the coexistence region, i.e., the $i + p$ mixed phase, exists in the system. There is no compensation temperature in the system for Figs. 3(b)–(d).

In our method, namely Glauber-type stochastic dynamics, one cannot write the free energy expression; hence we could not discern the unstable and/or metastable solutions from the stable equations by using the free energy expression, especially by comparing the free energy values of these solutions and as well as investigating the free energy surfaces. However, what we have done; since at absolute zero temperature $|M_\sigma|$ and $|M_S|$ should be 0.5 and 1 or zero, respectively. Thus in the numerical calculation if $|M_\sigma| = 0.5$ and $|M_S| = 1$

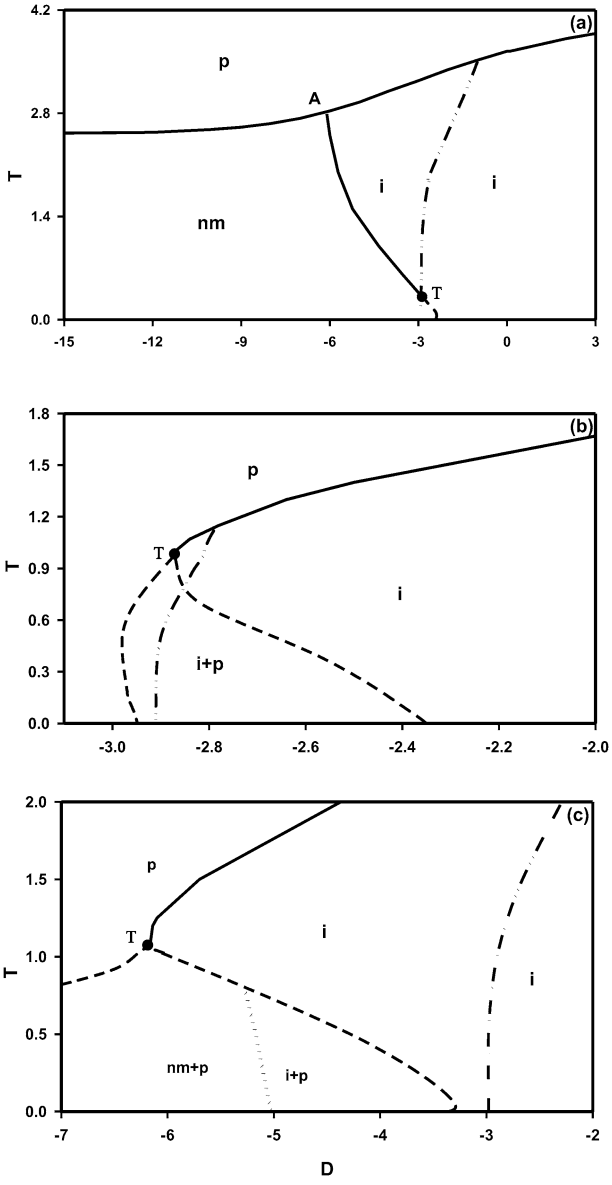

Fig. 4 Dynamic phase diagrams of the mixed spin Ising ferrimagnetic model in the (D, T) plane. *Dashed* and *solid lines* are the dynamic first- and second-order phase boundaries, respectively. *The dash-dot-dot line* illustrates the compensation temperatures. The special points are the dynamic tricritical point with filled circle and the dynamic multicritical point (A). *The dotted line* is an ordered line smoothly mediating, with no phase transition, between the $nm + p$ and $i + p$ mixed phases. (**a**) $J_1 = -1.0$, $J_2 = 5.0$, $J_3 = 0.9$ and $H_0 = 0.1$, (**b**) $J_1 = -1.0$, $J_2 = 1.1$, $J_3 = 0.9$ and $H_0 = 2.0$, (**c**) $J_1 = -1.0$, $J_2 = 4.0$, $J_3 = 0.98$ and $H_0 = 3.0$

or zero at absolute zero temperature, these solutions are considered, in general, as stable solutions, otherwise the solutions are the unstable and/or metastable. We should also mention that some of the unstable and/or metastable solutions of $|M_\sigma|$ and $|M_S|$ may take 0.5, and 1 or zero values, respectively, at absolute zero temperature. In this case, these solutions are the artifact of the method due to the limitations such that the free energy expression cannot be written.

Since we have obtained DPT points and compensation temperatures, we can now present the dynamic phase diagrams of the system. The calculated phase diagrams in the (D, T) plane is presented in Fig. 4 and (J_2, T), $(-J_3, T)$, (D, J_2) and $(D, -J_3)$ planes are presented

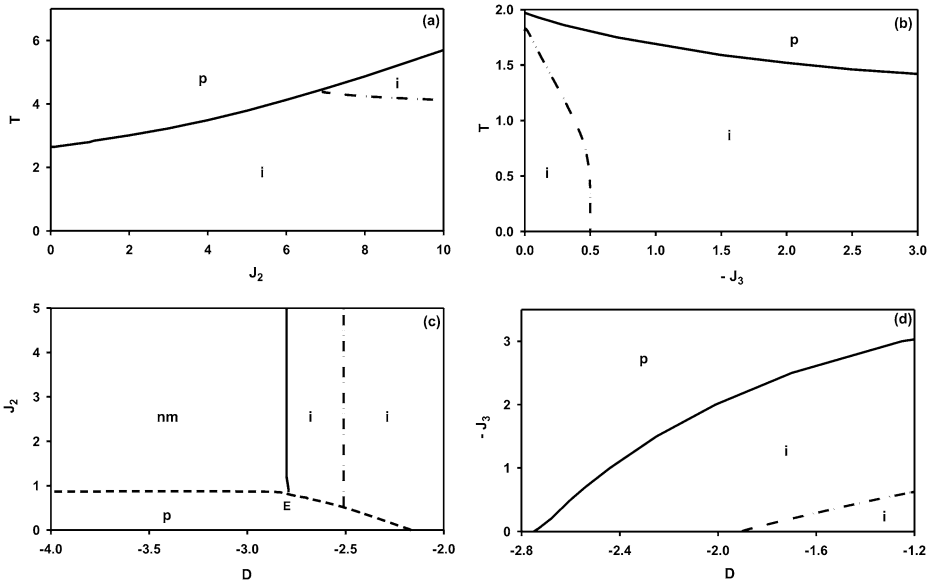

Fig. 5 Same as Fig. 4, but (**a**) In (J_2, T) plane for $J_1 = -1.0$, $J_3 = 0.9$, $H_0 = 0.5$ and $D = 2.0$; (**b**) In $(-J_3, T)$ plane for $J_1 = -1.0$, $J_2 = 2.0$, $H_0 = 0.1$ and $D = -1.5$; (**c**) In (D, J_2) plane for $J_1 = -1.0$, $J_3 = 0.5$, $T = 0.1$ and $H_0 = 0.7$; (**d**) $J_1 = -1.0$, $J_2 = 1.1$, $H_0 = 0.1$ and $T = 1.0$

in Fig. 5 for varies values of interaction parameters. In these dynamic phase diagrams, the solid, dashed and dash-dot-dot lines represent the second-order, first-order phase transitions temperatures and the compensation temperatures, respectively. The dynamic tricritical point is denoted by a filled circle.

Figure 4 illustrates the dynamic phase diagrams in (D, T) plane and three main topological different types of phase diagrams are seen. The following phenomena have been observed from these phase diagrams. (1) The system contains the p, nm and i fundamental phases, and the $i + p$ and $nm + p$ mixed phases. (2) The system exhibits the dynamic multicritical point (A), seen in Fig. 4(a). (3) Figure 4(b) exhibits a reentrant behavior, but Figs. 4(a) and (c) do not. (4) In Fig. 4(c), the $nm + p$ mixed phase exists at low values of T and D and the dotted line is an ordered line smoothly mediating, with no phase transition, between two mixed phases, namely the $nm + p$ and $i + p$. We have found a similar behavior to the one seen in the phase diagrams of the two-sublattice spin-3/2 Ising model by using the renormalization group calculation [20], the mixed ferrimagnetic ternary alloy on the Bethe lattice [21], the mixed spin-2 and spin-5/2 [17], the mixed ferrimagnetic ternary system with a single-ion anisotropy on the Bethe lattice [22] and the mixed spin-1/2 and spin-S Ising model on a bathroom tile (4–8) lattice [23]. We should also mention that these dynamic phase diagrams are new phase diagrams which have been obtained in this system.

We also calculate the dynamic phase diagrams including the compensation behaviors in the (J_2, T), $(-J_3, T)$, (D, J_2) and $(D, -J_3)$ planes, and five, four, three and two main topological different types of dynamic phase diagrams are found, respectively. Since the most of the phase diagrams in these planes can be readily obtained from the phase diagram in (D, T) plane, especially high and low values of D. We present only one interesting phase diagram, that cannot be obtained readily from the phase diagrams in the (D, T) plane, in each plane, seen in Figs. 5(a)–(d). The phase diagram is constructed for $J_1 = -1$, $J_3 = 0.9$,

$H_0 = 0.5$ and $D = 2.0$, and is presented in Fig. 5(a) that the system exhibits the p and i fundamental phases. In this phase diagram, the dynamic phase boundary is only a second-order phase transition line, which separates the p phase from the i phase. Figure 5(a) contains the compensation temperatures, but does not illustrate the dynamic tricritical behavior. The similar phase diagram with Fig. 5(a) was also obtained in the mixed spin-1/2 and spin-1 system without the oscillating magnetic field [1] and the mixed spin-2 and spin-5/2 system in the presence of the oscillating magnetic field [17]. The phase diagram for $J_1 = -1$, $J_2 = 2$, $H_0 = 0.1$ and $D = -1.5$, are shown in Fig. 5(b) and this phase diagram is similar to that in Fig. 5(a). Figure 5(c) shows the phase diagrams in the (D, J_2) plane for $J_1 = -1.0$, $J_3 = 0.5$, $T = 0.1$ and $H_0 = 0.7$. The phase diagram does not illustrate the dynamic tricritical behavior and it does not contain mixed phases. The dynamic phase boundary between the i and nm is a second-order phase transition line and between the i and p is first-order phase transition line. Moreover, the system shows the critical end point (E). The phase diagram is constructed for $J_1 = -1$, $J_2 = 1.1$, $H_0 = 0.1$ and $T = 1$, and it is presented in Fig. 5(d). The p and i fundamental phases occur in the system and the dynamic phase boundary is a second-order phase transition line. Thus, these phase diagrams of Figs. 5(b)–(d) are only observed in this system.

On the other hand, the comparison of our results with the mixed spin-1/2 and spin-1 Ising system in equilibrium [24], same set of parameters but different lattice, namely a Bethe lattice, is as follows: (1) Dynamic phase diagrams of the mixed spin-1/2 and spin-1 Ising system depending on the values of interaction parameters illustrate the tricritical and reentrant behaviors, but static or equilibrium phase diagrams of the mixed spin-1/2 and spin-1 Ising system illustrates only the tricritical behavior. (2) Dynamic phase diagrams of the system have the i, p and nm fundamental phases, but static phase diagrams of the system only contain the i and p fundamental phases. (3) Dynamic phase diagrams of the system exhibit the $i + p$ and $nm + p$ mixed phases, but static phase diagrams of the system do not exhibit any mixed phase. (4) Dynamic phase diagrams of the system contain special points such as the critical end point (E) and the multicritical point (A), but the static phase diagrams of the system do not contain any special point. Thus, the dynamic phase diagrams of the system give more complex and richer phase diagrams than static phase diagrams of the system. Similary, the result for dynamical compensation points was compared with the relevant result for the static compensation point of the mixed spin-1/2 and 1 Ising system [25], same set of parameters but different lattice, namely a Bethe lattice, is as follow: Dynamic phase diagrams of the mixed spin-1/2 and spin-1 Ising system display the N-type compensation temperature depending on the values of interaction parameters, same as [1], but equilibrium phase diagrams of the system illustrate N-type, P-type and L-type compensation temperatures.

It should be mentioned that there is a strong possibility that at least some of the first-order transition lines and also dynamic special points are very likely artifacts of the method due to its limitations such as the free energy expression cannot be written and the correlation of spin fluctuations have not been considered. However, this study suggests that the kinetic mixed spin-1/2 and spin-1 Ising ferrimagnetic model has an interesting dynamic behavior. We hope that our detailed theoretical investigation may stimulate further works to study the DPT points and compensation temperatures, and present the dynamic phase diagrams in the mixed Ising model by using more accurate techniques such as dynamic Monte Carlo (MC) simulations. It should be also noted that although the results of the dynamic MC method is rather reliable, it is always constrained by the speed of computer; hence our results will be instructive for the time consuming process of searching critical behavior while using the dynamic MC simulations.

In summary, we have studied, within a mean-field approach, the stationary states of the kinetic mixed spin-1/2 and spin-1 Ising model in the presence of a time-dependent oscillating external magnetic field on a hexagonal lattice. We find that the system displays the N-type compensation temperature as in [1], namely, the system in the absence of the oscillating magnetic field. The system under the oscillating magnetic field exhibits the tricritical temperature and reentrant behaviors, but the system in the absence of the oscillating magnetic field does not. The dynamic phase diagrams contain the critical end point (E) and the multicritical point (A) special points in which the phase diagrams in [1] do not. Therefore, the system in the oscillating magnetic field gives more richer and different topological types of phase diagrams.

Acknowledgements This work was supported by the Scientific and Technological Research Council of Turkey (TÜBİTAK, Grant No: 107T533) and Erciyes University Research Fund (Grant No: FBA-06-01).

References

1. Godoy, M., Leite, V.S., Fiqueiredo, W.: Mixed-spin Ising model and compensation temperature. Phys. Rev. B **69**, 054428 (2004)
2. Gatteshi, D., Kahn, O., Miller, J.S., Palacio, F. (eds.): Magnetic Molecular Materials. NATO ASI Series. Kluwer Academic, Dordrecht (1991)
3. Bahmad, L., Benyoussef, A., Kenz, A.E.: Mean field study of the mixed Ising model in a random crystal field. Physica A **387**, 825 (2008) ;
4. Bobàk, A., Abubrig, O.F., Horvàth, D.: Magnetic properties of a mixed ferro-ferrimagnetic ternary alloy. Physica A **312**, 187 (2002)
5. Buendía, G.M., Hurtado, N.: Numerical study of a three-dimensional mixed Ising ferrimagnet in the presence of a external field. Phys. Status Solidi B **220**, 959 (2000)
6. Boechat, B., Filgueiras, R.A., Cordeiro, C., Branco, N.S.: Renormalization-group magnetization of a ferrimagnetic Ising system. Physica A **304**, 429 (2002)
7. Albayrak, E.: Exact calculation of the magnetic susceptibility and the specific heat of the mixed spin-1/2 and spin-1 system on the Bethe lattice. Int. J. Mod. Phys. B **18**, 3959 (2004)
8. Buendía, G.M., Novotny, M.A.: Numerical study of a mixed Ising ferromagnetic system. J. Phys.: Condens. Matter **9**, 5951 (1997)
9. Monsuripur, M.: Magnetization reversal, coercivity and the process of thermomagnetic recording in thin films of amorphous rare earth-transition metal alloys. J. Appl. Phys. **61**, 1580 (1987)
10. Hansen, P.: Thermomagnetic switching in amorphous rare-earth transition metal alloys. J. Appl. Phys. **62**, 216 (1987)
11. Machado, E., Buendía, G.M.: Metastability and compensation temperatures for a mixed Ising ferrimagnetic system. Phys. Rev. B **68**, 224411 (2003)
12. Bobák, A., Jaščur, M.: Ferrimagnetism in diluted mixed Ising spin systems. Phys. Rev. B **51**, 11533 (1995)
13. Aydiner, E., Yüksel, Y., Kis-Cam, E., Polat, H.: Dependence on dilution of critical and compensation temperatures of a two-dimensional mixed spin-1/2 and spin-1 system. J. Magn. Magn. Mater. **321**, 3193 (2009)
14. Glauber, R.J.: Time-dependent statistics of the Ising model. J. Math. Phys. **4**, 294 (1963)
15. Leite, V.S., Godoy, M., Fiqueiredo, W.: Finite-size effects and compensation temperature of a ferrimagnetic small particle. Phys. Rev. B **71**, 094427 (2005)
16. Keskin, M., Deviren, B., Canko, O.: Dynamic compensation temperature in the mixed spin-1/2 and spin-3/2 Ising model in an oscillating field on alternate layers of hexagonal lattice. IEEE Trans. Magn. **45**, 2640 (2009)
17. Keskin, M., Ertaş, M.: Existence of a dynamic compensation temperature of a mixed spin-2 and spin-5/2 Ising ferrimagnetic system in an oscillating field. Phys. Rev. E **80**, 061140 (2009)
18. Néel, L.: Magnetic properties of ferrites: Ferrimagnetism and antiferromagnetism. Ann. Phys. **3**, 137 (1948)
19. Chikazumi, S.: Physics of Ferromagnetism. Oxford University Press, London (1997)
20. Renklioğlu, B., Berker, A.N., Keskin, M.: Stepwise positional and orientational ordering in the spin-3/2 Ising model: A plastic crystal phase diagram from renormalization-group theory. Phys. Rev. Lett. (to be submitted)

21. Canko, O., Deviren, B., Keskin, M.: Critical behavior of a mixed ferrimagnetic ternary alloy on the Bethe lattice. JETP Lett. **87**, 633 (2008)
22. Deviren, B., Canko, O., Keskin, M.: Magnetic properties of the mixed ferrimagnetic ternary systems with a single-ion anisotropy on the Bethe lattice. J. Magn. Magn. Mater. **321**, 1231 (2009)
23. Strečka, J.: Exact results of a mixed spin-1/2 and spin-S Ising model on a bathroom tile (4–8) lattice: Effect of uniaxial single-ion anisotropy. Physica A **360**, 379 (2006)
24. Albayrak, E., Yılmaz, S.: Spin-1/2 and spin-1 Ising model with crystal field on a bilayer Bethe lattice. Physica A **387**, 1173 (2008)
25. Ekiz, C.: Influence of anisotropic crystal-field on a ferromagnetic mixed-spin bilayer system. Physica A **387**, 1185 (2008)